Suspensions of colloidal plates in a nematic liquid crystal: a small angle x-ray scattering study

2004 J. Phys.: Condens. Matter 16 2479

(http://iopscience.iop.org/0953-8984/16/15/002)

INSTITUTE OF PHYSICS PUBLISHING JOURNAL OF PHYSICS: CONDENSED MATTER

J. Phys.: Condens. Matter **16** (2004) 2479–2495 PII: S0953-8984(04)73847-3

Suspensions of colloidal plates in a nematic liquid crystal: a small angle x-ray scattering study

Claire Pizzey[1], **Susanne Klein**[2], **Edward Leach**[2], **Jeroen S van Duijneveldt**[1] **and Robert M Richardson**[3]

[1] School of Chemistry, Cantock's Close, University of Bristol, Bristol BS8 1TS, UK
[2] HP Laboratories, Filton Road, Stoke Gifford, Bristol BS34 8QZ, UK
[3] H H Wills Physics Laboratory, Tyndall Avenue, University of Bristol, Bristol BS8 1TL, UK

Received 23 December 2003
Published 2 April 2004
Online at stacks.iop.org/JPhysCM/16/2479
DOI: 10.1088/0953-8984/16/15/002

Abstract

Suspensions of anisometric particles in the nematic phase of a liquid crystalline host solvent were prepared. We chose Claytone AF, a commercial quaternary ammonium surfactant treated montmorillonite, with an aspect ratio of up to 1:2000, and dimethyldioctadecylammonium bromide treated Laponite, with an aspect ratio of 1:8 as the dispersed particles. K15, a nematogenic compound (also known as 5CB), was the dispersing medium. The suspensions were characterized by small angle x-ray scattering (SAXS). The liquid crystal delaminates the clays well, but the scattering curves from Claytone suspensions have prominent first and second order pseudo Bragg peaks, indicating that stacking of clay plates has occurred. We report a model for fitting SAXS data based on Hosemann's theory for suspensions of plane parallel sheets.

1. Introduction

Most reported liquid crystal colloids involve the suspension of spherical particles, such as colloidal silica or polymer lattices, in a liquid crystalline host (Stark 2001). Spheres, treated with a polymeric stabilizer, cause the formation of topological defects and disruption of the nematic matrix. The matrix acts to expel the spheres to minimize the energy in the system, and a defect stabilized network structure, called a 'filled nematic', results (Kreuzer and Eidenschink 1996). We are interested in suspensions that do not flocculate when cooled from the isotropic into the nematic phase, i.e. where the particles are not expelled. Plates cause fewer topological defects, and with careful tuning, a good dispersion that minimizes the potential for defect structures may be prepared (Kawasumi *et al* 1999, 1996). These systems could exhibit interesting ordering and phase behaviour as compared to the pure host material. It is therefore crucial to characterize the interaction of the dispersed particles with the dispersing medium. The maximum dimensions of the plates are approximately 2 μm for Claytone and much less (0.03 μm) for Laponite. These are too small to lead to conclusive results when the suspensions

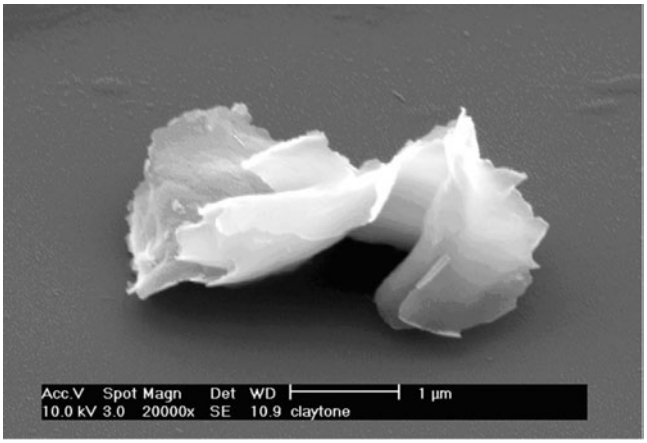

Figure 1. Electron micrograph of Claytone AF. The image shows clearly that the plates are rather flexible structures.

are inspected under a polarization microscope. Light scattering is not suitable when the liquid crystal is in the nematic phase, as the signal generated by nematic domains cannot be easily differentiated from the signal generated by the dispersed particles. Small angle x-ray scattering (SAXS) is the preferred characterization method. The apparatus we have used has a scattering vector-range from 0.03 to 0.6 $Å^{-1}$ so we can probe a size range between 10 and 200 Å. Although this does not allow determination of the diameter of suspended Claytone or even Laponite plates, we are able to see whether the clays delaminate completely or form periodic structures.

2. Sample preparation

In order to limit the defect formation, a low molecular weight surfactant, rather than a polymeric surface treatment, was chosen to stabilize the particles in the suspension against mutual attractive forces and subsequent aggregation.

The two types of clay plates used are of similar chemical structure but differ greatly in aspect ratio. Claytone AF (Southern Clay Products) is a surface treated natural montmorillonite clay with a thickness of approximately 1 nm and a range of diameters from 500 to 2000 nm (van Olphen 1977) (see figure 1). With this high aspect ratio the particles are not rigid plates but have some flexibility, as can be seen in the micrograph. Claytone is commercially pre-treated with dihydrogenated tallow, a surfactant mixture, the main component of which is dimethyldioctadecylammonium bromide (DODAB) (Ho *et al* 2001) to give stable suspensions in non-aqueous solvents. The treated clay was cleaned repeatedly with a 40/60 mixture of propanol and water (ultra pure, Millipore) to remove excess surfactant, dried under vacuum and finely ground prior to use.

Laponite RD (Rockwood Additives) is a synthetic hectorite type clay with a thickness of approximately 1 nm and a diameter of 25 nm (Rockwood Additives 2003). Laponite was totally dispersed in water (1 g, 1% w/w) by stirring for 24 h prior to surfactant treatment. The surfactant DODAB (Acros Chemicals, used as received) was added in dilute solution in an 80:20 water:propanol mix to give 100% coverage using the cation exchange capacity (CEC) calculated in Cione *et al* (1998). The treated clay was cleaned by repeated washing and was subsequently dried under vacuum to remove all traces of water (Jordan 1949). The particles were finely ground with an agate pestle and mortar and dried prior to suspension in the isotropic phase of the liquid crystal. Inspection by scanning electron microscopy (SEM)

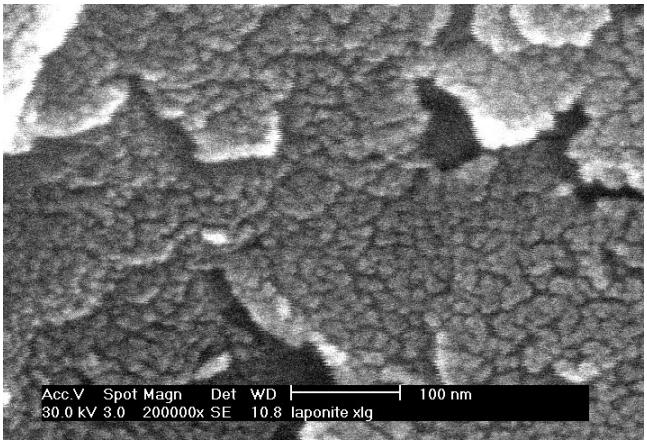

Figure 2. Electron micrograph of Laponite. The image shows aggregates and smaller structures which could be single particles since their maximum dimension is smaller than 50 nm.

shows that Laponite when delaminated consists of plates with diameters smaller than 100 nm (see figure 2).

Laponite has a strong tendency to form films when suspended in water and then dried on a clean piece of glass. To get a glimpse of single plates under the SEM we used very dilute suspensions (1 part of Laponite in 1000 parts of water) and sprayed these onto a heated glass slide (180 °C) to avoid droplet formation and hence agglomeration of the Laponite particles. Even after this treatment, single plates could only be seen in between agglomerates. These single plates have a diameter, d, of less than 100 nm, confirming the literature values of $10\,\text{nm} < d < 40\,\text{nm}$ (Balnois *et al* 2003) and $20\,\text{nm} < d < 95\,\text{nm}$ (Zhivkov and Stoylov 2002).

The liquid crystal chosen was K15 (4-pentyl-4′-cyanobiphenyl, Merck, used as received) due to its high purity and room temperature nematic phase. K15 is a widely used liquid crystal with a nematic–isotropic transition temperature (T_{NI}) of 35 °C (BDH 1986). It is well known that this transition temperature is easily shifted by trace impurities. Adding clean, dry stabilized clay does not shift T_{NI} (although we have previously observed a decrease of T_{NI} for solvent contaminated samples) and therefore we conclude that the stabilizer is irreversibly attached to the plates and does not dissolve into the liquid crystal. The particles do not behave as chemical contaminants. A shift in T_{NI} in the suspensions would therefore be indicative of contamination in the sample.

The clay suspensions were prepared by adding the dry powder to the isotropic phase of the liquid crystal and stirring for 15 min. This was followed by 6–7 h of sonication, degassing under vacuum and then cooling to the nematic phase. The particles did not sediment, and the suspension was then stable for up to 24 h, after which time flocculation was observed. The sample then developed two discrete layers, one particle poor and the other particle rich with an open floc structure (see figure 3). The aggregates were easily broken up; 15 min of stirring at approximately 40 °C restored a good suspension.

3. Small angle x-ray scattering

SAXS measurements over a temperature range from 25 to 40 °C were performed at the University of Bristol Physics Department. The diffraction measurements were made using copper Kα x-rays (averaged $\lambda = 0.154$ nm), from a sealed tube with other wavelengths

Figure 3. Phase separation after 40 h. From left to right: 0.5, 1, 2, 3, 4 and 5 wt% of DODAB stabilized Laponite in K15.

removed using a nickel filter and a graphite monochromator. The diffraction pattern was detected using a multi-wire area detector (Bateman *et al* 1987). It was placed at 840 mm from the sample with an evacuated path so that a Q (scattering vector) range from 0.03 to 0.6 Å^{-1} was covered. The sample to detector distance was calibrated using a silver behenate standard (Huang *et al* 1993). The suspensions were filled into Lindemann glass capillaries (diameter 2 mm, wall thickness 0.01 mm) which had been flattened to give a path length of ∼1 mm for the x-ray beam. The samples were cooled from the isotropic phase in a ∼0.5 T magnetic field.

The measured counts were corrected for the efficiency of each pixel by dividing the data by the counts from a ^{55}Fe radioactive source, which gave an isotropic flood of x-rays. The transmission of the samples was determined during the data acquisition runs by taking the counts from the main beam (after passing through an attenuating beam stop) on the detector. The transmission was determined as the ratio of these counts with and without the sample in the beam.

The scattering from the liquid or liquid crystal host was subtracted from the scattering from the dispersions using the formula

$$I_{\text{correct}} = \frac{I_{\text{L+P}}}{T_{\text{L+P}} R_{\text{L+P}}} - \frac{I_{\text{L}}}{T_{\text{L}} R_{\text{L}}}, \tag{1}$$

where $I_{\text{L+P}}$ is the intensity from the dispersion (liquid + particles) in a sample tube, $T_{\text{L+P}}$ is the transmission of the dispersion in a sample tube, and $R_{\text{L+P}}$ is the length of the run. I_{L}, T_{L} and R_{L} are the corresponding quantities for a sample of the pure dispersion medium (liquid only). Since the dispersion only contains a few per cent of clay and the sample tubes were nominally the same thickness, this formula gives a reasonable correction for the scattering from the liquid host and the container. After the background correction, the data were azimuthally averaged in order to improve statistics and make the scattering from the isotropic and nematic phases comparable (figure 4).

4. Theoretical background

This section outlines the background theory for the scattering from suspensions of plate-like objects. In particular, we consider how the proportion of plates that are stacked and the characteristics of the stacks influence the scattering.

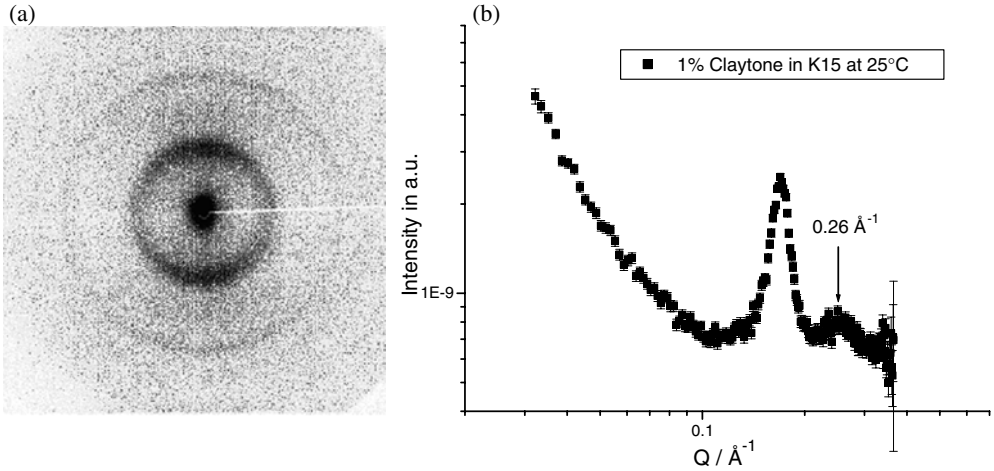

Figure 4. Scattering from 1% Claytone in K15 at 25 °C with vertical director in the form of (a) detector image and (b) the azimuthally averaged scattering from a vertical band as a function of the scattering vector, Q. No detector efficiency or background correction has been applied. The peak corresponding to 0.26 Å^{-1} is due to K15. The other two peaks are respectively first and second order pseudo Bragg peaks from the suspended particles.

We have assumed that the particles are either single plates of clay or stacks of plates with some intervening surfactant and/or host. For sufficiently dilute suspensions (typically <1% by volume) inter-particle interference may be neglected. The scattering from an anisotropic particle may be calculated from the square of the single particle structure factor, averaged over all orientations of the particle with respect to the scattering vector, **Q**. For simplicity we will consider disc-shaped plates although it turns out that, in the Q range of interest, the scattering is insensitive to the in-plane shape of the plates. The structure factor of a particle with cylindrical symmetry is given as the product of a radial and an axial structure factor:

$$F(\mathbf{Q}) = F_{\mathrm{a}}(Q\cos\theta)F_{\mathrm{r}}(Q\sin\theta), \tag{2}$$

where θ is the angle between the cylindrical axis and the scattering vector, **Q**. The scattering from an assembly of perfectly aligned identical particles depends on the number of particles illuminated by the incident beam, the electron density contrast between a particle and the solvent, $\Delta\rho$, and the square of the structure factor:

$$I(\mathbf{Q}) = N_{\mathrm{P}}\Delta\rho^2 F_{\mathrm{a}}^2(Q\cos\theta)F_{\mathrm{r}}^2(Q\cos\theta). \tag{3}$$

For samples where the cylindrical axis may point in any direction at random, the scattering depends on the orientational average of the structure factor:

$$I(Q) = N_{\mathrm{P}}\Delta\rho^2 \int_0^{\pi/2} F_{\mathrm{a}}^2(Q\cos\theta)F_{\mathrm{r}}^2(Q\cos\theta)\sin\theta\,\mathrm{d}\theta. \tag{4}$$

For discs, the radial structure factor is given by an expression containing the first order Bessel function, J_1:

$$F_{\mathrm{r}}(Q\sin\theta) = \pi r^2 \frac{2J_1(Qr\sin\theta)}{Qr\sin\theta}, \tag{5}$$

where r is the radius. At low Q, this expression tends to πr^2, the cross-sectional area of the disc. For single discs, the axial structure factor is given by the expression

$$F_{\mathrm{a}}(Q\cos\theta) = h\frac{\sin(Q(h/2)\cos\theta)}{Q(h/2)\cos\theta}, \tag{6}$$

where h is the thickness of the disc. At low Q, this expression tends to h, the thickness of the disc. For isolated discs, the scattering can be calculated by performing the average in equation (4) numerically (Lin *et al* 1987). However, in this work, the pseudo Bragg peaks in the data suggested that the discs were stacked to some extent. We therefore consider possible models for the stacking.

Initially we considered the most general model available for the stacking of the discs. For stacks of discs, the structure factor depends on the number of discs in a stack, M, the disc or 'hard' phase thickness, h, and the gap or 'soft' solvent phase thickness, s. In addition, there may be some variation in the thickness of the 'hard' phase and the 'soft' phase. We assumed that these variations have Gaussian distributions characterized by the standard deviations, σ_h and σ_s. In this case, the axial structure factor may be calculated using the expressions given by Hosemann (Hosemann and Bagchi 1962):

$$F_a(Q\cos\theta) = I_B(Q\cos\theta) + I_C(Q\cos\theta). \tag{7}$$

The first term, known as the 'Babinet' term, produces pseudo Bragg peaks at Q values corresponding to $2\pi/(h+s)$ and tends to zero at zero Q. The second term, known as the 'crystal' term, is the coherent scattering from the whole stack and tends to $(Mh)^2$ at low Q. These two terms are given by the expressions

$$\begin{aligned} I_B(Q\cos\theta) &= \frac{2M}{Q^2}\,\mathrm{Re}\left(\frac{(1-F_h)(1-F_s)}{1-F_hF_s}\right) \\ I_C(Q\cos\theta) &= \frac{2}{Q^2}\,\mathrm{Re}\left\{F_s\left(\frac{1-F_h}{1-F_sF_h}\right)^2[1-(F_sF_h)^M]\right\}, \end{aligned} \tag{8}$$

where F_h and F_s are the Fourier transforms of the distributions of 'hard' and 'soft' phase thicknesses, and for Gaussian distributions they are given by the expressions

$$\begin{aligned} F_h(Q) &= \exp(-\mathrm{i}Qh)\exp\left(-\frac{Q^2\sigma_h^2}{2}\right) \\ F_s(Q) &= \exp(-\mathrm{i}Qs)\exp\left(-\frac{Q^2\sigma_s^2}{2}\right). \end{aligned} \tag{9}$$

The final expression for the scattered intensity for a collection of stacks of M discs becomes

$$I_M(Q) = N_P\Delta\rho^2V_D^2\int_0^{\pi/2}\left(\frac{2J_1(Qr\sin\theta)}{Qr\sin\theta}\right)^2\left(\frac{I_B(Q\cos\theta)+I_C(Q\cos\theta)}{h^2}\right)\sin\theta\,\mathrm{d}\theta \tag{10}$$

where the volume of a single disc, V_D, has been factored out. The integral may be evaluated numerically and the effect of polydispersity of the disc radius and the number of discs in a stack may be included by numerical averaging over a Gaussian distribution of r and M. However, for $Q \geqslant \pi/r$ the Bessel function only contributes to the integral for $Qr\sin\theta \sim 0$, and the integration over θ introduces a factor of $2\pi/(AQ^2)$, where A is the area of the disc (Kratky and Porod 1948). Since $Q(\mathrm{min}) \sim 0.03$ Å^{-1} and $r \geqslant 100$ Å, all the data in this work satisfy the condition that $Q \geqslant \pi/r$, and so the following approximate formula was used. The polydispersity of the number, M, in a stack is retained and the angle brackets in equation (11) below indicate an average over a distribution of M with standard deviation σ_M:

$$I_M(Q) \approx \frac{N_P\Delta\rho^2Ah^2 2\pi}{Q^2}\,\frac{I_B(Q\cos\theta)+\langle I_C(Q\cos\theta)\rangle_M}{h^2}. \tag{11}$$

Comparison of lines (b) and (d) in figure 5 gives an indication of the quality of this 'large disc' approximation. It is excellent except that the troughs between the peaks are slightly underestimated and, as expected, it breaks down at low Q.

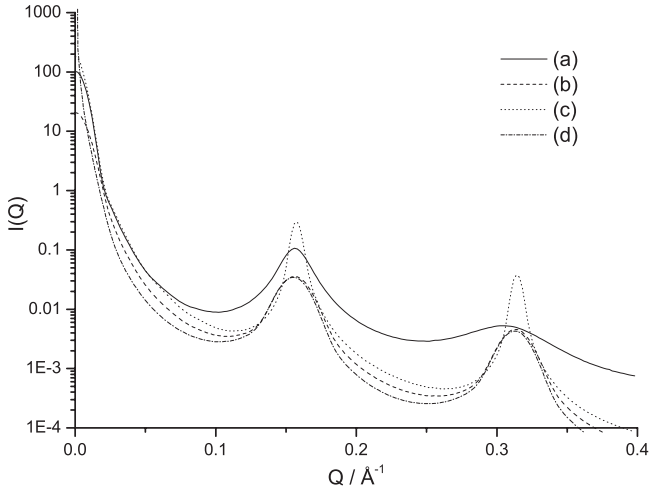

Figure 5. Scattering intensity expected from (a) the Hosemann model with a fluctuating gap between the plates and the regular but finite stack with (b) 4 ± 2 plates and (c) 12 ± 6 plates in the stack. For (a)–(c), the plate radius is 200 Å with a polydispersity of 40% and a plate thickness of 10 Å. For (d), the stacking is the same as for (b) but it is calculated in the large disc approximation.

It is useful to evaluate equation (10) for some typical parameter values in order to guide our interpretation of the scattering data. First we consider the interpretation of the widths of the pseudo Bragg peaks. Figure 5(a) shows the scattering calculated for a stack of 10 ± 2 discs of identical thickness ($h = 10$ Å, $\sigma_h = 0$) separated by a soft phase layer of mean thickness $s = 30$ Å and standard deviation $\sigma_s = 5$ Å. It shows peaks at $Q = n(2\pi/(h+s)) = n \cdot 0.157$ Å^{-1} as expected from a structure with a period of 40 Å. It illustrates that the width of the pseudo Bragg peaks increases with their order as is expected for this type of disorder. Inspection of the experimental data (see for example figures 8–11) indicates that the first and second order peaks are of nearly the same width, so variability in the soft (or hard) layers' spacing is not the primary cause of the large peak width. The other possible source of broadening is the finite number of discs in the stack. Figure 5(b) also shows the scattering calculated for a stack of 4 ± 2 discs of identical thickness ($h = 10$ Å, $\sigma_h = 0$) separated by a soft phase layer of identical thickness (i.e. $s = 30$ Å, $\sigma_s = 0$). It can be seen that the peaks have the same widths and so this suggests that the origin of the peak widths in the experimental data is the small number of discs in a stack. Figure 5(c) shows the scattering calculated for a stack of 12 ± 2 discs of identical thickness ($h = 10$ Å, $\sigma_h = 0$) separated by a soft phase layer of identical thickness (i.e. $s = 30$ Å, $\sigma_s = 0$) which has narrower peaks, illustrating that the peak width is inversely proportional to the number in the stack irrespective of the details of the model. More precisely, the full width at half maximum of the pseudo Bragg peaks, ΔQ, is given by $\Delta Q \sim M^{-1} Q_{001}$, where Q_{001} is the position of the first order peak. This is essentially a description of a finite, one-dimensional crystal, and the scattering may be formulated more simply using formulae analogous to a diffraction grating with M slits:

$$I_M(Q) \approx \frac{N_P \Delta\rho^2 A h^2 2\pi}{Q^2} \left(\frac{\sin Qh/2}{Qh/2}\right)^2 \left\langle \left(\frac{\sin MQd/2}{\sin Qd/2}\right)^2 \right\rangle_M , \tag{12}$$

where $d = h + s$ is the total thickness of a hard and a soft layer and the angle brackets indicate an average over a distribution of M with standard deviation σ_M.

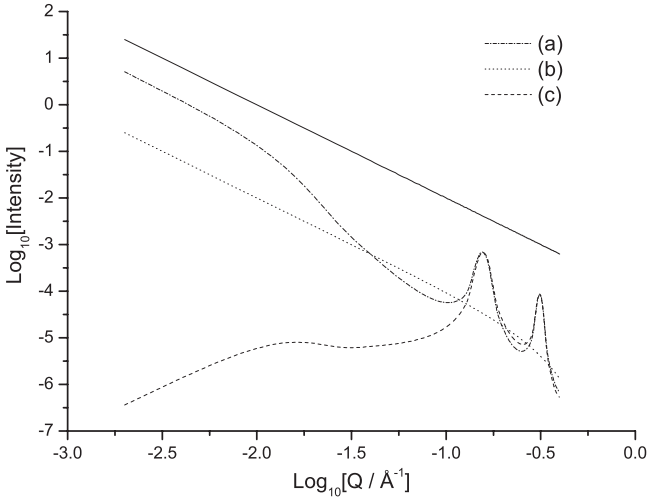

Figure 6. The intensity expected from (a) stacks of four discs, (b) single discs, and (c) stacks of four with the mean electron density of the stack matched to the surroundings. A line of slope $= -2$ is shown for comparison.

For a single thin disc the scattering for $2\pi/h \geqslant Q \geqslant \pi/r$ follows a Q^{-2} power law decay. Figure 6 shows the scattering expected from single discs (from equation (10) with $M = 1$) and stacks of four discs (from equation (10) with $M = 4$) as a log–log plot. It demonstrates that the initial Q^{-2} power law decay is characteristic of both single and stacked discs, provided the overall shape remains highly anisotropic. However, the stacked discs show a greater intensity near $Q = 0$, and there is a region where the scattering from the stack falls more rapidly than as Q^{-2}. The absence of such a feature in the scattering would suggest that a sample comprised predominantly single delaminated discs. However, some of our scattering data show pseudo Bragg peaks, suggesting stacked discs but no such extra increase in the scattering at $Q \sim 0$. This leads us to consider other structural features that might suppress the intensity at $Q \sim 0$. The heights of the maxima described by the finite one-dimensional crystal $\left(\frac{\sin MQd/2}{\sin Qd/2}\right)^2$ term in equation (12) are the same. However, the physical origins of the peaks are different. The zero order peak (at $Q \sim 0$) results from the contrast between the crystal and its surroundings, and is similar to the 'crystal' term in the Hosemann formulation. The higher order peaks are pseudo Bragg peaks resulting from the internal periodic structure of the crystal, and arise from 'Babinet' terms in the Hosemann formulation. If the crystal were surrounded by material whose electron density was the same as its average electron density, the zero order peak would have zero intensity. In order to describe the scattering from stacks of plates that are embedded in a larger aggregate of similar composition, a second term has been included so that the contrast between a crystal and its surroundings can be adjusted:

$$I_M(Q) \approx \frac{N_P \Delta\rho^2 A h^2 2\pi}{Q^2} \left(\frac{\sin Qh/2}{Qh/2}\right)^2 \langle \sin^2 MQd/2 \rangle_M \left(\frac{1}{\sin Qd/2} - \frac{2\varphi}{Qd}\right)^2. \tag{13}$$

In this equation, φ is used to adjust the electron density of the surroundings of any particular stack of plates. If the mean electron density of a stack relative to the pure solvent is $\Delta\bar{\rho} = \Delta\rho h/(h+s)$, then the above formula assumes that the mean scattering electron density relative to pure solvent of the surroundings of the stack is $\varphi\Delta\bar{\rho}$, as illustrated in figure 7. In a very dilute suspension $\varphi = 0$ is expected, and the zero order peak would have its full intensity. In an aggregate of many crystals at random orientations, $\varphi = 1$ is expected, and the zero order

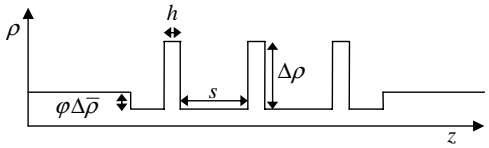

Figure 7. Schematic diagram of electron density as a function of distance, z, perpendicular to the plane of a stack of three plates.

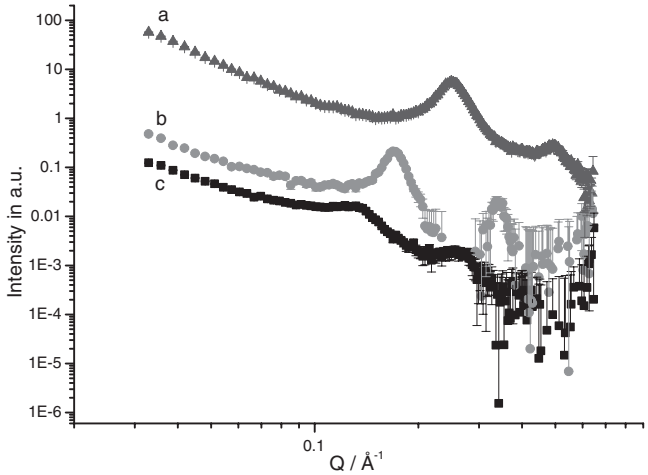

Figure 8. Scattering data from (a) Claytone dry powder, (b) 1% suspension of Claytone in K15 multiplied by 10, and (c) 1% suspension in toluene.

peak would have zero intensity. Figures 6(a) and (c) shows two extremes with $\varphi = 0$ and 1, respectively.

In general, it is possible that a suspension of clay may contain two types of particle: single delaminated discs and stacks of discs. The surroundings of the two types of particle might also be different, with the possibilities ranging from pure solvent to similar particles as described above. In this case, the scattered intensity is given by the weighted sum of the scattering from stacks and scattering from single discs:

$$I(Q) \approx \frac{\Delta\rho^2 A h^2 2\pi}{Q^2}\left(\frac{\sin Qh/2}{Qh/2}\right)\left(N_M\langle\sin^2 MQd/2\rangle_M\left(\frac{1}{\sin Qd/2}-\frac{2\varphi_M}{Qd}\right)^2 + N_1\sin^2 Qd/2\left(\frac{1}{\sin Qd/2}-\frac{2\varphi_1}{Qd}\right)^2\right), \tag{14}$$

where the subscripts M and 1 refer to the stacks of M discs and the single delaminated discs respectively. For fitting the scattering data in this work, we have assumed that $\varphi_M = \varphi_1$ and combined the plate volume, contrast and incident intensity into a single scaling factor, S:

$$I(Q) \approx \frac{S}{Q^2}\left(\frac{\sin Qh/2}{Qh/2}\right)\left((1-x)(\langle\sin^2 MQd/2\rangle_M + x\sin^2 Qd/2)\left(\frac{1}{\sin Qd/2}-\frac{2\varphi}{Qd}\right)^2\right), \tag{15}$$

where x is the fraction of the particles that are single discs rather than stacks.

The scattering from the suspensions of clay has been analysed using equation (15). It describes the model discussed above, where the stacks are regular but with a small number of

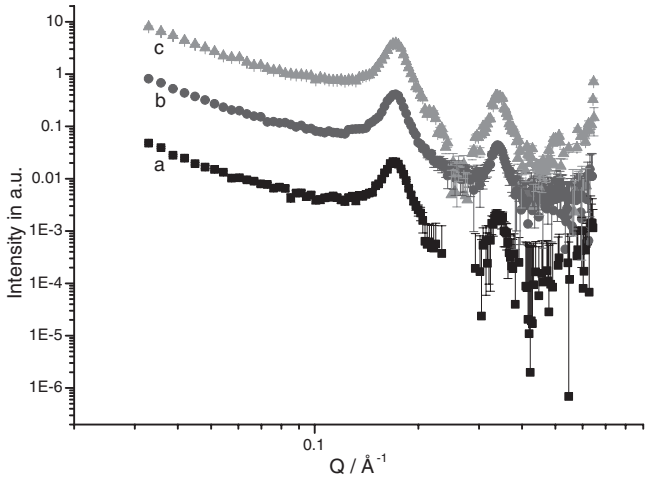

Figure 9. Temperature scan of 1% Claytone AF in K15. Time elapsed between the first measurement (25 °C heating) and the last (25 °C cooling): 15 h. The curves are shifted for clarity. (a) 25 °C heating, (b) 40 °C times 10, (c) 25 °C cooling times 100.

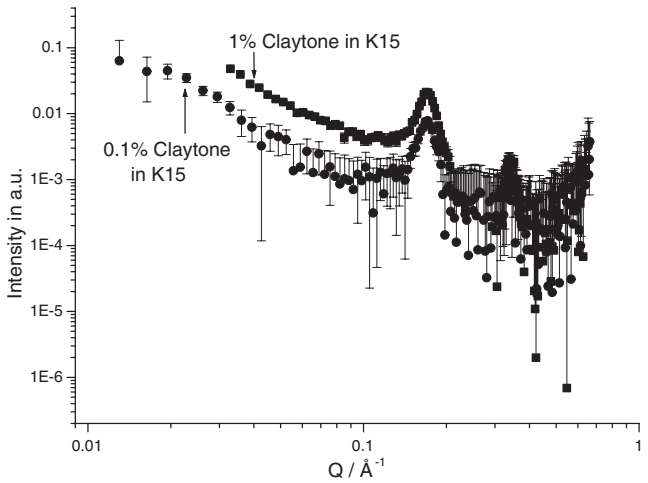

Figure 10. Scattering from 0.1% and 1% Claytone in K15.

plates rather than stacks with more plates with variable spacing. The seven model parameters $S, h, d, M, \sigma_M, \varphi$ and x have been adjusted to fit the shape of the scattering data. Initial values were estimated as follows. For scattering data with a Q^{-2} behaviour at low Q, it was expected that $x \sim 1$. The value of the repeat distance, d, was estimated from $d \sim 2\pi/Q_{001}$, where Q_{001} is the position of the first order pseudo Bragg peak. The number of plates in the stacks was estimated using $M \approx \Delta Q/Q_{001}$, where ΔQ is the full width at half maximum of the first order peak. The plate thickness was taken at 10 Å, in accordance with the known structure of the clays (van Olphen 1977, Rockwood Additives 2003).

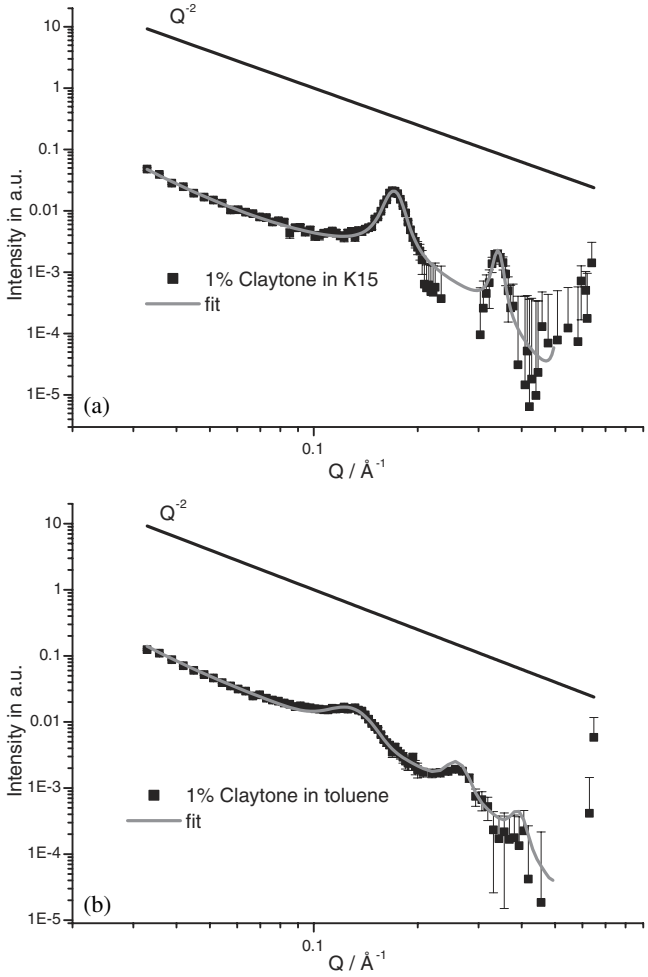

Figure 11. (a) 1% Claytone in K15, data and fit. (b) 1% Claytone in toluene, data and fit. A line of slope −2 is included for comparison.

5. Results

5.1. Claytone suspensions

As expected, the scattering from dry Claytone powder is most intense. With a high particle concentration and a high electron density difference between clay and air, the intensity is at least two orders of magnitudes larger than that for the suspensions.

The peak from dry Claytone powder implies a repeat distance of 25 Å, which is consistent with 10 Å thick discs (van Olphen 1977) with surfactant layers of about 15 Å thickness. Comparison of scattering data from Claytone AF powder with dispersions in K15 and toluene shows that the pseudo Bragg peaks are not caused by non-dispersed powder. On forming a suspension, we observe a clear increase in the repeat distance of the plates, from 25 Å in the powder to 37 Å in K15 and 48 Å in toluene. Assuming a plate thickness of 10 Å, this indicates that the gap between the plate surfaces has increased from 15 to 27 Å in K15, and 38 Å in

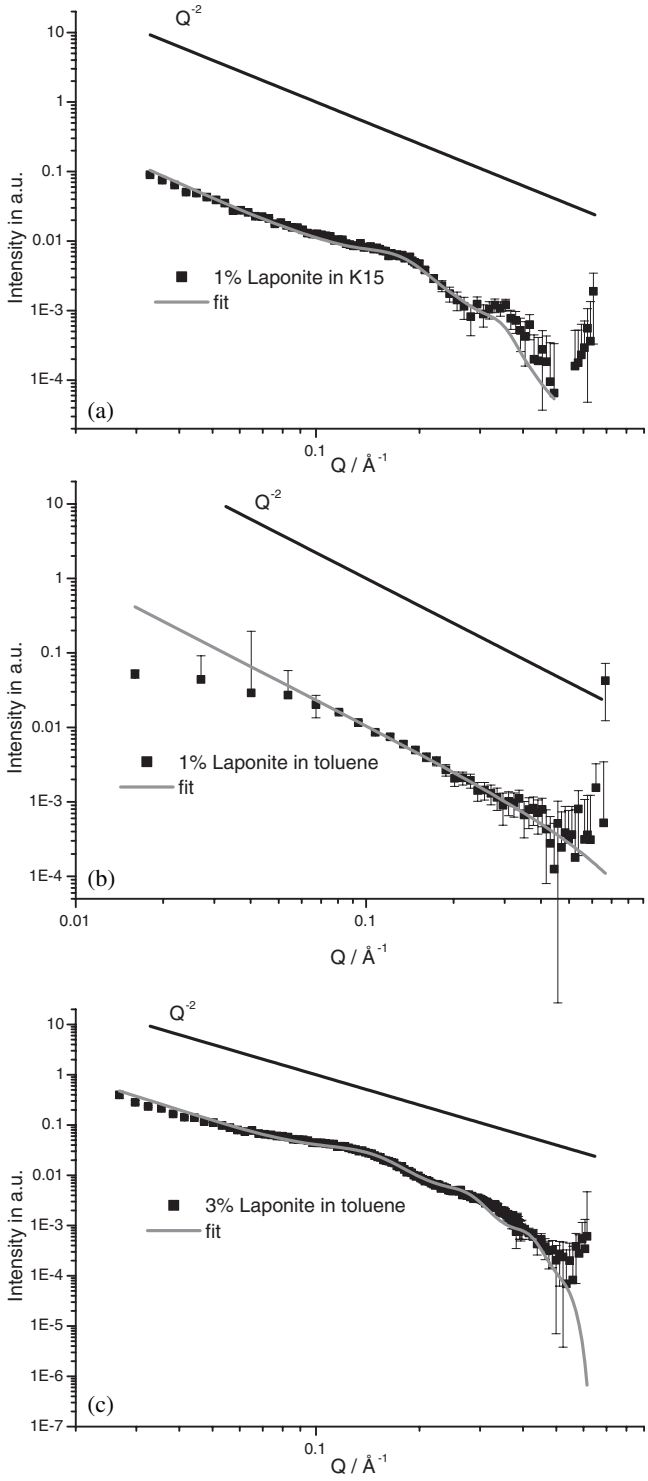

Figure 12. Laponite suspensions. (a) 1% Laponite in K15, data and fit. (b) 1% Laponite in toluene, data and fit. (c) 3% Laponite in toluene, data and fit. A line of slope −2 is included for comparison.

toluene. This suggests that the aggregates in the powder are delaminated by the solvents but subsequently self-assemble into ordered stacks within the dispersion. This effect is most prominent in K15, but there is also some evidence of stacking in toluene dispersions.

Comparing the suspension in toluene with the suspension in K15, we find that the peak from the toluene suspension has shifted to lower Q. It is broader and less prominent. This indicates that the clay is well delaminated and the stacks forming within the dispersion have fewer sheets. A gap of 38 Å suggests that the surfactant stabilizer chains are nearly extended (extended length ∼22 Å, rough estimate for the surfactant mixture). This suggests that the gap contains both surfactant and toluene which swells the surfactant. Powder and toluene data agree well with literature values of, respectively, 24.3 and 46.5 Å (Ho *et al* 2001).

The K15 molecules have a length of about 17 Å when extended, and they have a strong tendency to associate into antiparallel dimers (length 24 Å) in the bulk (Leadbetter *et al* 1975). From the size of the gap we infer that the aggregate is formed by a single layer of K15 molecules intermixing with two extended chains of the steric stabilizer.

The narrower peaks indicate that the nematic liquid crystal matrix promotes larger stacks than toluene. This may result from the interaction of the K15 molecules with the surfactant on adjacent plates which would tend to 'hold' the plates together.

When the liquid crystal is heated from the nematic into the isotropic phase, no observable change in the peak position takes place (see figure 9). This implies that the bonding between the plates that is, to some extent, mediated by the K15, is independent of the state of bulk K15 surrounding the plates. The inter-plate adhesion is so strong that it cannot be overcome by thermal agitation, even when the bulk is in the isotropic phase. It is remarkable that the inter-plate distance is independent of temperature. This suggests that the stacks are a rather stable state of aggregation. Inspection of the scattering data in figures 8 and 9 indicates that the first and second order pseudo Bragg peaks have a very similar width. As discussed in the theoretical background, this means that the stacks are finite but contain regularly spaced plates with no significant variability in the plate thickness or the inter-plate gaps.

The change in intensity between the first and last measurement in figure 9 can be understood in terms of the experimental schedule. At each temperature there was a 1 h wait time followed by a 2 h data acquisition time. A temperature sequence of 25, 30, 35, 30 and 25 °C was run so that 15 h elapsed between the first and the last measurement. Since the suspensions are only stable up to ∼24 h and aggregates at the bottom of the vial were generally observed after 15 h, it is clear that some change of the numbers of particles in the beam takes place. With shorter measurement times it would be possible to correlate floc formation with the scattering signal from the aggregating suspension. In a future paper we will report the results from these observations.

It seems that the monolayer of K15 molecules between the plates is a stable state, as scattering from more dilute suspensions (figure 10) does not show a shift in the peak position to lower Q.

In figure 10 the signal from the clay is very weak in the 0.1% curve and noisy compared to the 1% curve. However, the first order peak is still in the same position. This implies that the number of stacks has decreased but the spacing between the plates in the stack has not changed.

To show that our theoretical model describes our experimental system, we have fitted the scattering data from Claytone and Laponite suspensions in two different host solvents using equation (15). This fitting allows us to confirm our model and to determine values for the stack height and plate spacing from the data.

As there are no discernible differences in the peak position between the scattering from the suspension of different concentrations and temperatures, we consider only the case of 1% w/w clay at 25 °C for fitting purposes.

Table 1. Fit parameters for all fits shown for Claytone.

Parameter	1% Claytone in K15	1% Claytone in toluene
Plate thickness, h (Å)	10 ± 1	10 ± 1
Periodicity, $h + s$ (Å)	37 ± 0.4	48 ± 1
Soft phase thickness, s (Å)	27 ± 1.4	38 ± 2
No. of plates in stack, M	5 ± 1	2 ± 0
Standard deviation of no. of plates, σ_M	2 ± 1	1 ± 0
Percentage of single plates in suspension $\frac{x}{x+(1-x)M} \times 100$ (%)	33 ± 5	67 ± 5
Volume fraction of stacks in solvent surrounding a given stack, φ	0.35 ± 0.5	0.02 ± 0.02

Figure 11 shows clearly that at low Q, i.e. $Q < 0.1$ Å^{-1}, the scattering data follow a Q^{-2} power law decay characteristic of both single and stacked discs. However, there is no step with an exponent greater than 2, as shown in figure 6. Since the pseudo Bragg peaks indicate the presence of stacks, this suggests that the mean electron density of the stacks is matched by the surrounding. The pseudo Bragg peaks in the region $0.1 < Q < 0.4$ Å^{-1} are fitted assuming a combination of free 'large' single discs and free stacks of 'large' discs (equation (15)). The model is in reasonable agreement with the data. However, it is not completely satisfactory for the K15 suspensions. The observed scattering at $Q \sim 0.25$ Å^{-1} is negative, and hence not shown in the graph. Since this is the region where the nematic peak occurs, it is possible that this peak has been reduced by the presence of the clay plates. Background subtraction of pure K15 overcompensates using equation (1) for the peak, and leads to an unrealistically low intensity in that region.

We start fitting equation (15) to the data by assuming a fixed plate thickness of 10 Å and a periodicity of 35 Å (K15 suspensions) and 45 Å (toluene suspension) calculated from the first order peak positions. The thickness of the clay plates is fixed, since the model is not very sensitive to variation in the thickness of the hard phase. The value of 10 Å has been confirmed in the literature (Cione *et al* 1998). The number of plates is estimated by the full half-width of the first maximum in the scattering data divided by the first order peak position. These parameters are allowed to vary, and the best fit is found by least squares fitting to the data. The proportion of single plates relative to the stacks in the system is a parameter which changes the height of the peaks relative to the Q^{-2} decay line. As mentioned earlier, the model described by equation (15) assumes that the standard deviation on the soft phase and hard phase are zero, since the peak width is the same for the first and second order peaks. Including variations in the thickness of the soft phase or hard phase would make the second order peak relatively broad and diminish its height.

The best fits for the scattering data are shown in figure 11, and the parameter values for these fits are given in table 1. The dimer length of K15 is 24 Å, and so an inter-plate separation of 27 Å is consistent with the model of two extended surfactant chains interlocking with a single layer of K15 dimers. The ordering influence of K15 is most visible in the percentage of single clay plates in the suspension. Only 33% of the clay present in suspension is in the form of free individual platelets. The rest exist in stacks of about 5 ± 2 plates.

In the case of the toluene suspensions, the situation is quite different. There are fewer plates in the stacks, 2 compared to 5, the gap between the plates has increased from 27 to 38 Å, and most of the particles in suspension are free single plates (67%), indicating less overall order imposed on the system. This demonstrates clearly the influence of the solvent molecular structure on the nature of the dispersion.

Table 2. Fit parameters for all fits shown for Laponite.

Parameter	1% Laponite in K15	1% Laponite in toluene	3% Laponite in toluene
Plate thickness, h (Å)	10 ± 1	10 ± 1	10 ± 1
Periodicity, $h + s$ (Å)	37 ± 2	—	52 ± 7
Soft phase thickness, s (Å)	27 ± 3	—	42 ± 8
No. of plates in stack, M	2–3	—	1–2
Standard deviation of no. of plates, σ_M	1–2	—	0–1
Percentage of single plates in suspension $\frac{x}{x+(1-x)M} \times 100$ (%)	90 ± 5	100	90 ± 5
Volume fraction of stacks in solvent surrounding a given stack, φ	0.31 ± 0.04	0	0.34 ± 0.04

The fitting program is based on a least square fit which does not lead to satisfactory results when all the parameters are refined simultaneously. The fits are achieved by manual intervention, i.e. the quality of the fits is judged by eye at first as the parameters are changed. The deviations given in the tables are not standard deviations in the mathematical sense. They describe the range of values for which the fits appear to be of equal quality. Some parameters are correlated, for example the average number of plates in a stack, M, and its standard deviation, σ_M. The fit changes very little when M or σ_M vary, as long as their sum stays constant. When the scattering data show well defined peaks, the range of possible values for the periodicity is narrow, but for featureless curves the fit becomes rather insensitive to this parameter. In all cases the range of parameters in the tables has been estimated by repeated trial and error while holding some parameters fixed at different values and allowing the others to refine.

5.2. Laponite suspensions

In this case the plates used have approximately the same thickness as the Claytone plates; however, they are much smaller in diameter. This difference in diameter also gives rise to a different structural behaviour; the Laponite plates may be considered to be rigid. The steric stabilizer on the surface of the Claytone does not greatly alter the aspect ratio; however, using the same stabilizer on Laponite changes the overall shape of the particle. The aspect ratio decreases from 1:26 (untreated) to 1:8 (surface treated). This means that the particle is now effectively more like an ellipsoid and less like a disc.

Despite the fact that the particles are smaller, they have a greater tendency to aggregate than the Claytone plates. This can be observed when the suspension is placed in a thin cell (a 2 mm diameter capillary or between microscope slides). Large open flocs start to form in less than 1 h, with complete phase separation occurring after 24 h. Claytone suspensions also sediment and phase separate after 24–36 h, but do not form these large open flocs.

As in the Claytone suspensions, the scattering data from Laponite suspensions do not change with variation in temperature (from 25 to 40 °C) or concentration (from 0.1% w/w to 5% w/w). The pseudo Bragg peaks that are so prominent in the data for Claytone suspensions become much weaker (they almost disappear) for Laponite suspensions, giving featureless scattering data that are difficult to fit.

The data for K15 as solvent cannot be fitted by consideration of single plates only, as might be assumed from the absence of prominent peaks. Nevertheless, 90% of the plates are free delaminated discs, and the stacks consist of 2 ± 1 plates only, i.e. the stacking tendency is minimal.

Toluene delaminates the clay completely in the 1% suspension, and its scattering can be fitted by single plates alone. For the 3% suspension we can fit the data by assuming the similar periodicity as for Claytone but the stack size is 1 ± 1 plates; that is, we have mostly completely delaminated clay with the occasional pair of plates.

The fitting values in table 2 show that the Laponite behaves very differently from the Claytone. We know that in K15 open flocs are formed quite quickly, certainly within our measurement time (2 h), as this may be observed by visual inspection of the capillaries. Nevertheless, the fitting parameters, maximal 2 plates in a stack and 90% free discs, indicate that the flocculation does not involve an enhanced stacking. The flocs are probably aggregates of plates with random orientations.

6. Conclusions

The clay suspensions in K15 are not stable over long periods of time. This is probably due to limited compatibility between the surfactant stabilizer and the liquid crystalline host. The suspensions in toluene are stable, and they provide a useful comparison. Further work will focus on refining this system to achieve better stabilization of the particles in the liquid crystalline medium to give longer term stability.

Nevertheless, the suspensions are sufficiently stable for analysis to give insight into the behaviour of anisometric particles in an anisotropic host. Plates with a greater aspect ratio, in this case Claytone, have shown a strong tendency to self-organize into stacks; this effect is most prominent in the case of the liquid crystal suspensions where 67% of all plates are in stacks with $\sim$5 sheets. This effect may also be observed in the toluene suspensions, but to a much lesser extent, with only 33% of all plates being in stacks. The increased tendency of K15 to form stacks as compared to the small molecule solvent toluene suggest that the larger K15 molecules enhance the interaction between the plates. Since the effect was observed above and below the clearing temperature, it does not appear to be a result of the interaction with the surrounding matrix. The approximate equality of the widths of the first and second order peaks confirms that there is negligible variability in the inter-plate gaps, which supports the suggestion that the stacks are formed as a result of strong inter-plate interaction, mediated by the solvent molecules and the stabilizer layer.

Stack formation is a frequently observed phenomenon in suspensions where montmorillonite is the suspended particle. Determination of the number of stacks in a suspension has not previously been attempted, but the numbers of plates in a stack in isotropic dispersing media are similar to our results. Numbers given in the literature vary with solvent and surface treatment from 1 (Ho *et al* 2001), 3 (Shang *et al* 2002) up to 6 (Hanley and Muzny 2003). For K15 solvent, the gap between the plates in a stack, 26–27 Å, appears to be independent of temperature, concentration and size of dispersed platelets. This merits further investigation. Small angle neutron scattering could give us detailed information about the arrangement of molecules at and around the plate surface because contrast variation may be used.

Laponite, chemically similar to Claytone but with a much smaller aspect ratio, lacks the strong tendency to form stacks. The 1% toluene solution showed no pseudo Bragg peaks, suggesting that the clay was completely delaminated. In order to detect any stack formation in toluene at all, we have fitted data from 3% suspensions where pseudo Bragg peaks just emerge and indicate spacing of 52 Å, similar to the spacing for Claytone in toluene. In K15 we find only pairs of plates, again with the same spacing as for Claytone, and only 10% of the platelets are in these stacks. Even after flocculation, at the end of our runs, the peaks have neither shifted nor increased in intensity, indicating that the flocs are aggregates of randomly oriented plates.

Acknowledgments

We would like to thank Steve Bodiley for his assistance performing SEM measurements. One of the authors (CP) would like to acknowledge the financial support of the EPSRC and Hewlett-Packard as part of the IMPACT Faraday Partnership.

References

Balnois E *et al* 2003 *Langmuir* **19** 6633–7
Bateman J E *et al* 1987 *Nucl. Instrum. Methods Phys. Res.* A **259** 506–20
BDH Product Information 1986
Cione A P P *et al* 1998 *J. Colloid Interface Sci.* **198** 106–12
Hanley H J M and Muzny C D 2003 *Langmuir* **19** 5575–80
Ho D L *et al* 2001 *Chem. Mater.* **13** 1923–31
Hosemann R and Bagchi S N 1962 *Direct Analysis of Diffraction by Matter* (Amsterdam: North-Holland)
Huang T C *et al* 1993 *J. Appl. Crystallogr.* **26** 180–4
Jordan J W 1949 *J. Phys. Colloid Chem.* **53** 294–306
Kawasumi M *et al* 1996 *Mol. Cryst. Liq. Cryst.* **281** 91–103
Kawasumi M *et al* 1999 *Appl. Clay Sci.* **15** 93–108
Kratky O and Porod G 1948 *Acta Phys. Austriaca* **2** 133
Kreuzer M and Eidenschink R 1996 Filled nematics *Liquid Crystals in Complex Geometries* ed G P Crawford (London: Taylor and Francis)
Leadbetter A J, Richardson R M and Colling C N 1975 *J. Physique Coll.* **36** C1 37–43
Lin T L *et al* 1987 *J. Phys. Chem.* **91** 406–13
Rockwood Additives Product Information 2003
Shang C *et al* 2002 *Soil Sci. Soc. Am. J.* **66** 1225–30
Stark H 2001 *Phys. Rep.* **351** 387–474
van Olphen H 1977 *An Introduction to Clay Colloid Chemistry* 2nd edn (New York: Wiley)
Zhivkov A M and Stoylov S P 2002 *Colloids Surf.* A **209** 315–8